Probabilistic centroid moment tensor inversions using geologically constrained priors Application to induced earthquakes in the Groningen gas field, the Netherlands

Masfara, La Ode Marzujriban; Weemstra, Cornelis; Cullison, Thomas

DOI
10.1190/image2023-3910056.1

Publication date
2023

Document Version
Final published version

Published in
SEG Technical Program Expanded Abstracts

Probabilistic centroid moment tensor inversions using geologically constrained priors: application to induced earthquakes in the Groningen gas field, the Netherlands

La Ode Marzujriban Masfara, Cornelis Weemstra, TU Delft; Thomas Cullison, Stanford University*

SUMMARY

We use the Hamiltonian Monte Carlo (HMC) algorithm to estimate the posterior probability distribution of a number of earthquake source parameters. This distribution describes the probability of these parameters attaining a specific set of values. The efficiency of the HMC algorithm, however, can be improved through the formulation of a geologically constrained prior probability distribution. The primary objective of the presented study is, therefore, to assess the role of the prior probability in the application of the HMC algorithm to recordings of induced seismic events in the Groningen gas field.

INTRODUCTION

Earthquake source inversion is essential in studying earthquakes because it provides quantitative characteristics of the earthquake's source (e.g., location, focal mechanism, and magnitude). Applied to induced seismicity in the Groningen gas field, it can be used to monitor the field. To obtain the uncertainty of source inversion, Bayesian algorithms are often employed. However, generic Markov chain Monte Carlo (McMC) algorithms (i.e., metropolis-hasting algorithms) are often computationally inefficient. The Hamiltonian Monte Carlo (HMC) algorithm is an alternative to those more generic McMC algorithms. It is an McMC algorithm known to be highly efficient when sampling high-dimensional model spaces. This is because, rather than sampling the model space in a random fashion, HMC uses Hamilton's equations to update its model estimates. We furthermore increase HMC's efficiency by linearizing the forward problem. Specifically, the relation between the hypocenter and the origin time of the event and the recorded particle displacements is linearized. In this study, we utilize this algorithm to estimate the source parameters of a 3.4 local magnitude induced earthquake located near the village of Westerwijtwerd, the Netherlands. The HMC algorithm is run iteratively and embedded in a specific workflow previously tested on synthetic recordings of induced seismic events (Masfara et al., 2022).

THEORY

Bayesian inference is the process of using Bayes' theorem to evaluate the probability of a hypothesis (or model) $\mathbf{m}$ given the observed data $\mathbf{d}$. Mathematically, the theorem is written as follows,

$$\rho(\mathbf{m}|\mathbf{d}) \propto \rho(\mathbf{d}|\mathbf{m})\rho(\mathbf{m}), \tag{1}$$

where $\rho(\mathbf{m}|\mathbf{d})$ is the posterior probability distribution, $\rho(\mathbf{d}|\mathbf{m})$ is the likelihood, and $\rho(\mathbf{m})$ the *a priori* known probability of each of the earthquake source parameters taking on a specific value. This is usually referred to as the prior probability distribution. In our case, $\mathbf{m}$ consists of a set of ten source parameters, which are the hypocenter (three coordinate components), moment tensor (six independent components), and origin time. Therefore, $\rho(\mathbf{m})$ represents the prior probability of those parameters. The likelihood $\rho(\mathbf{d}|\mathbf{m})$ quantifies the difference between observed and forward-modeled data. In our context, the observed data are the recorded particle displacements, whereas the forward modeled data are obtained by solving the forward problem, which involves the computation of the particle displacements given specific values for each of the ten model parameters and for an accurate (known) subsurface velocity model. We solve the forward problem by computing particle displacements $\mathbf{u}$ given a moment tensor source $\mathbf{M}$ (Aki and Richards, 2002)

$$u_i(\mathbf{x}_r,t) = \sum_{j,k=1}^{3} M_{jk}(t,T_0) * G_{ij,k}(\mathbf{x}_r;\mathbf{x}_a,t) \tag{2}$$

with subscript i indicating the direction along which the displacement is computed, whereas j and k are the other two coordinate directions. The (3D) position where the displacement is recorded is represented by $\mathbf{x}_r$, and the location of the moment tensor source is represented by $\mathbf{x}_a$. Furthermore, $\mathbf{G}$ is the Green's tensor (9 components), and a comma followed by a subscript represents a spatial derivative along that coordinate axis. Finally, the in-line asterisk $*$ represents temporal convolution and T_0 the origin time of the event.

Assuming Gaussian observational errors and a Gaussian distributed prior probability, equation 1 can be written as

$$\rho(\mathbf{m}|\mathbf{d}) \propto \exp\Bigg(-\frac{1}{2}\left(\mathbf{u}(\mathbf{m})-\mathbf{u}^{\text{obs}}\right)\mathbf{C}_d^{-1}\left(\mathbf{u}(\mathbf{m})-\mathbf{u}^{\text{obs}}\right) - \frac{1}{2}\left(\mathbf{m}-\mathbf{m}^0\right)\mathbf{C}_m^{-1}\left(\mathbf{m}-\mathbf{m}^0\right)\Bigg), \tag{3}$$

where $\mathbf{m}^0$ is the mean of the Gaussian prior probability with $\mathbf{C}_m$ and $\mathbf{C}_d$ being the model covariance and data covariance matrices, respectively. These covariance matrices quantify the uncertainties of the prior knowledge of the source parameters and the observed data, respectively.

Hamiltonian Monte Carlo

Several probabilistic algorithms are available for evaluating equation 3. The workflow we implement uses the HMC algorithm. HMC was derived from classical mechanics, applied to statistical mechanics (Betancourt, 2017), and considered one of the most efficient probabilistic algorithms. A generic McMC algorithm such as Metropolis-Hasting performs random exploration of the model space by proposing random models, which is often inefficient in high-dimensional spaces. This inefficiency is because the randomly proposed model is less likely to be accepted in high-dimensional model spaces. This is illustrated for a two-dimensional model space in Figure 1a. Instead

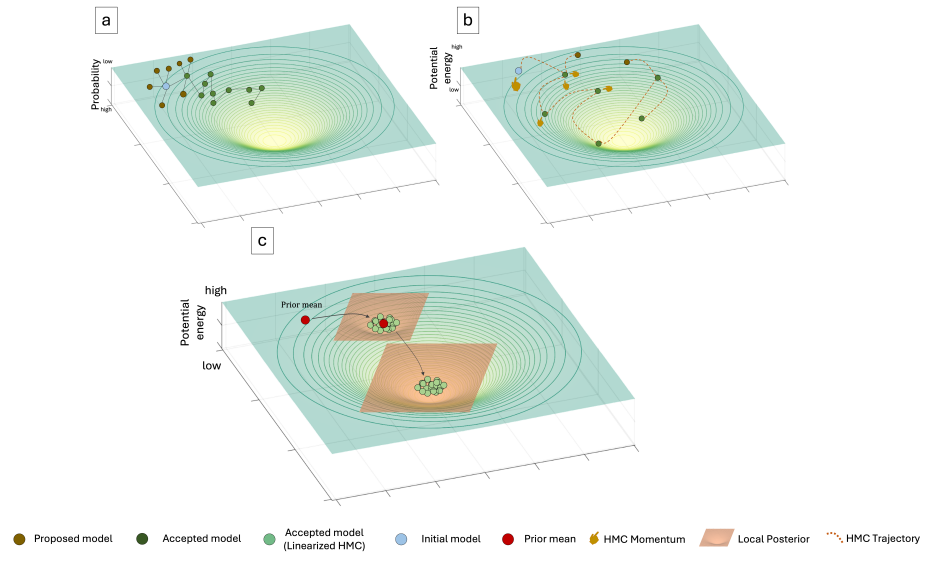

Figure 1: Illustration of Metropolis-Hasting algorithm (a), Hamiltonian Monte Carlo (b), and Hamiltonian Monte Carlo with a linearized forward model (c).

of being random, our implementation of HMC uses two quantities which facilitate sampling the more likely models (Masfara et al., 2022). These quantities are the potential energy U, as a function of $\rho(\mathbf{m}|\mathbf{d})$, and the kinetic energy K as a function of momentum vector $\mathbf{p}$

$$U(\mathbf{m}) = -\ln \rho(\mathbf{m} \mid \mathbf{d}) \tag{4}$$

$$K(\mathbf{p}) = \mathbf{p}^T \mathscr{M}^{-1} \mathbf{p}/2. \tag{5}$$

Combined, they form the Hamiltonian $H(\mathbf{m},\mathbf{p})$, which represents the total energy of a system (Neal et al., 2011), i.e.,

$$H(\mathbf{m},\mathbf{p}) = K(\mathbf{p}) + U(\mathbf{m}). \tag{6}$$

The mass matrix $\mathscr{M}$ in equation 5 can be seen as a tuning parameter that governs the amount of momentum applied during sampling, which then affects the length of the HMC's trajectory.

In application, HMC compares the Hamiltonian of a starting model $H(\mathbf{p},\mathbf{m})$ and the proposed model $H(\mathbf{p}(\tau),\mathbf{m}(\tau))$. The probability θ of accepting the proposed model is then computed using the metropolis rule

$$\theta = \min\left[1, \frac{\exp[-H(\mathbf{p}(\tau),\mathbf{m}(\tau))]}{\exp[-H(\mathbf{p},\mathbf{m})]}\right]. \tag{7}$$

The quantity τ is the "artificial time" used to "propagate" the initial model to the proposed model in phase space (Betancourt, 2017). When propagating the model, HMC uses Hamilton's equations to simultaneously update the model and momentum vectors and hence its potential and kinetic energy. As illustrated in Figure 1b, given an initial momentum vector (visualized using the pointing finger), solving Hamilton's equations will propagate the starting model to an area in phase space with low potential, which corresponds to a region of the model space with (relatively) high probability. Hamilton's equations, through the computation of the gradient of the potential energy $\mathrm{d}U/\mathrm{d}\mathbf{m}$ and the corresponding solution of Hamilton's equations, make the model vector "slide" through regions of phase space with constant H (Betancourt, 2017).

To speed up model exploration by the HMC algorithm, Fichtner and Simutė (2018) linearize equation 2 and use a prior while computing the posterior. This leads to the estimation of parameters that can be used to explore a "local" posterior. This exploration of the local posterior doesn't require the need for forward modeling per iteration, which is the evaluation of equation 2. Instead, it uses simple functions to approximate equation 3, given mean priors, which then eases the computation of Hamilton's equations. Illustrated in Figure 1c, the workflow we use implements this approach in multiple stages; that is, by updating its mean prior, using the mean of the "local posterior" as the new mean prior. However, this approach will not be effective if the initial prior mean is not located in the correct lobe, which is the case when sampling multi-modal spaces.

DATA

The detection of earthquakes in the Netherlands is mainly carried out by the Royal Netherlands Meteorological Institute (KNMI) using a local seismic network named the 'G-network'. The network has numerous borehole seismometers that provide high signal-to-noise ratio (SNR) recordings. The seismometers located at the bottom of the borehole (200 m depth), in particular, deliver high SNR recordings. The high quality of the recordings increases the accuracy of source parameter estimation in the area as previously shown by Willacy et al. (2019), and Smith et al. (2020). In this research, we use recordings of a 3.4 local magnitude earthquake near the village of Wester-

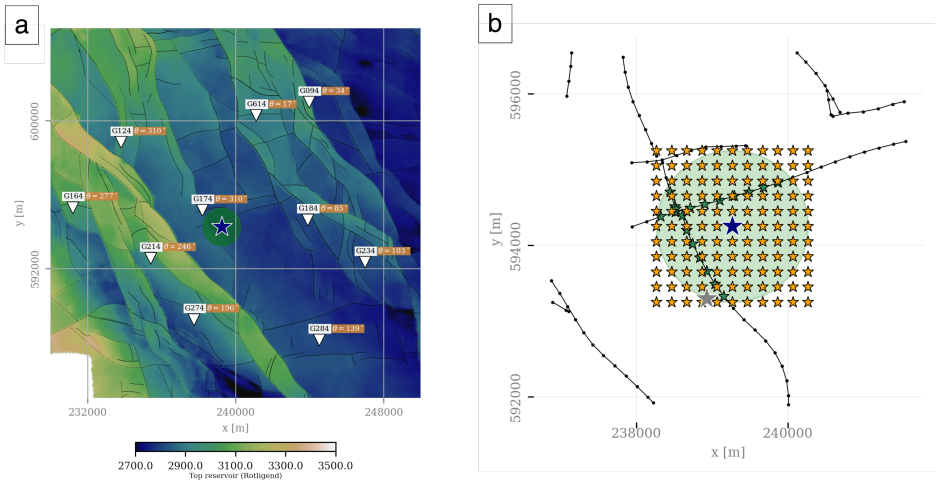

Figure 2: a) Location of the ten seismometers whose recordings were used in the inversion. b) Zoom of the area where the earthquake occurred. The white triangles represent KNMI seismometers. The blue, green, yellow, and gray stars represent the KNMI estimate of the epicenter, the initial epicenter prior means for scenario 1, the initial epicenter prior means for scenario 2, and the event's epicenter estimated by Dost et al. (2020).

wijtwerd in the province of Groningen. Specifically, we use the seismograms by the ten G-network seismometers represented by the white triangles shown in Figure 2a. In Figure 2a, we also plot the top reservoir of the Groningen gas field, the major subsurface faults intersecting the top reservoir, and the location of the epicenter estimated by the KNMI.

As discussed above, a sufficiently accurate initial prior probability is a requirement to sample the "correct" mode of the posterior. To ensure this, we generate multiple initial priors, as such avoiding only sampling local modes, and for that, we consider two scenarios. In the first scenario, the initial hypocenter prior means are based on the assumption that the earthquake nucleated on one of the existing (mapped) faults. The initial epicenter prior means are the result of lateral regular sampling of these faults (spacing of 200 m) within a circle of 1 km radius centered at the KNMI-derived epicenter (green stars in Figure 2b). As for the second scenario, we assume that the earthquake may not have nucleated on one of the existing (mapped) faults. Therefore, we create a grid of initial epicenter prior means, also centered at the KNMI-derived epicenter (yellow stars in Figure 2b). For each epicenter's prior mean, the depth prior mean is set at 3 km, which is the default KNMI estimation for all earthquake depths. For the moment tensor prior means, we use random values for each set, whereas, for origin time, the workflow will estimate the initial prior mean of origin time given each of the initial prior means for the hypocenter. For both scenarios, the epicenter prior means are depicted in Figure 2b. In total, in the first scenario, we have 15 initial prior means, and for the second, we have 121. Each of these prior means will be the start of a separate multi-stage HMC workflow, which each consists of a total of 20 stages, where each stage is an individual HMC chain associated with an updated prior and hence involves linearization of equation 2 about a new prior mean $\mathbf{m}^0$ (see also Masfara et al., 2022).

RESULTS

Using both defined scenarios, we run in total 136 multi-stage HMC workflows (i.e., 136 initial prior mean sets). The likelihood is computed using 2.5 s of P-wave signals in each case, i.e., the vector with observed data consists of three-component particle displacement recordings of 2.5 s by 10 borehole seismometers. For each workflow, we update the prior mean 20 times (20 stages). Of all samples by those 20 stages, for all different initial prior mean sets, we only collect samples from stages for which the variance reduction (e.g., Mustać and Tkalčić, 2016) exceeds 0.95. We compute this variance reduction with respect to the observed data by generating modeled data using the mean of the local posteriors (i.e., associated with the different stages). The marginal posterior probabilities derived from those samples are presented in Figure 3 for the first scenario and in Figure 4 for the second scenario. In both figures, in (a), we show the posterior for each model parameter, including their mean and standard deviation. In (b), we show the 2D posterior for the epicenter, which shows the probability of the epicenter peaks near a major fault. In fact, a bit closer to that fault than the hypocenter estimated by Dost et al. (2020) (represented by the gray star). The latter authors, however, employ a 1D velocity model, whereas we use a 3D velocity model (forward modeled seismograms were generated using SPECFEM, Komatitsch and Tromp, 2002). For both scenarios, given the mean of the moment tensors posterior probability, we find that the mean values for the strike, dip, and rake are 161, 70, and -100, respectively (normal faulting). Similarly, For the source mechanism, we obtain -19% and -29% as the mean value for its isotropic and compensated linear vector dipole components, respectively. The negative value in the isotropic components is often linked to the compaction in the reservoir layer due to the gas extraction in the Groningen gas field. All in all, for this presented case, the use of geological knowledge reduces the number of initial prior means. That is, a geologically-inspired

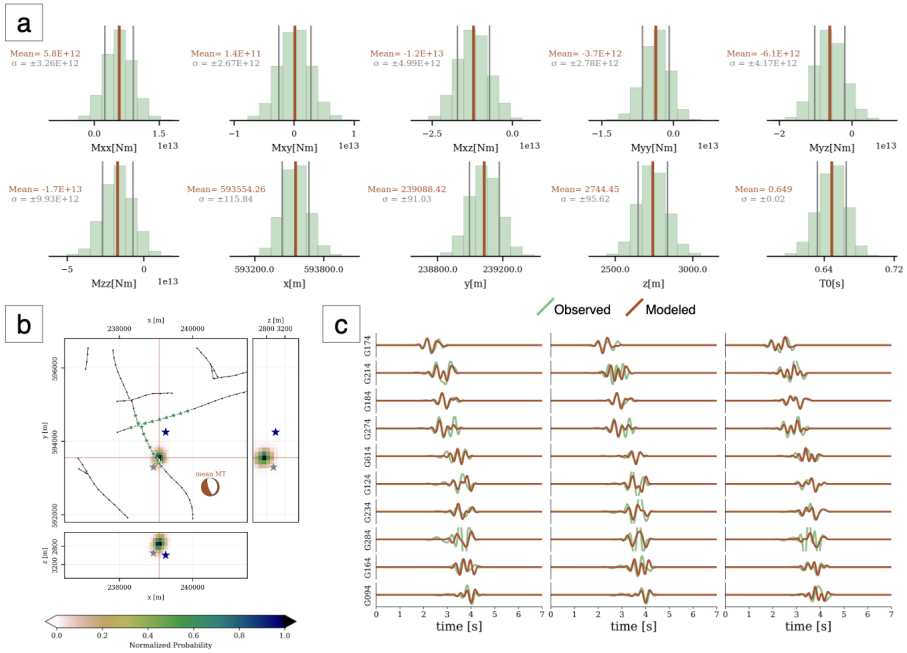

Figure 3: Results from using the HMC workflow for scenario 1. a) 1d marginal posterior density of each model parameter. b) 2d marginal posterior density for the epicenter. c) Comparison between observed signals and modeled signals using the posterior's mean value for each model parameter in a).

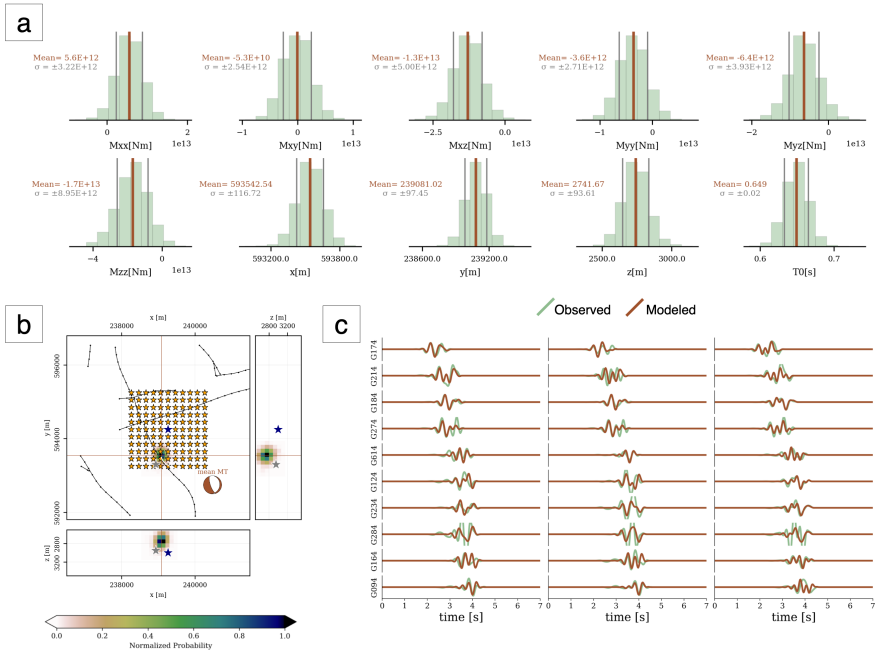

Figure 4: Results from using the HMC workflow for scenario 2. a), b), and c) are explained below Figure 3.

set of initial prior hypocenter means (fault-based approach) reduces the required computational resources compared to a more uniform set of initial prior means(i.e., grid approach).

ACKNOWLEDGMENTS

This research was (partially) funded by the NWO Science Domain (NWO – ENW) project DEEP.NL.2018.048.

10.1190/image2023-3910056.1

REFERENCES

Aki, K., and P. G. Richards, 2002, Quantitative seismology, 2nd ed.: University Science Books.

Betancourt, M., 2017, A conceptual introduction to Hamiltonian Monte Carlo: arXiv preprint arXiv:1701.02434.

Dost, B., A. van Stiphout, D. Kuhn, M. Kortekaas, E. Ruigrok, and S. Heimann, 2020, Probabilistic moment tensor inversion for hydrocarbon-induced seismicity in the groningen gas field, the netherlands, part 2: Application: Bulletin of the Seismological Society of America, **110**, 2112–2123, doi: https://doi.org/10.1785/0120200076.

Fichtner, A., and S. Simute, 2018, Hamiltonian Monte Carlo inversion of seismic sources in complex media: Journal of Geophysical Research: Solid Earth, **123**, 2984–2999, doi: https://doi.org/10.1002/2017JB015249.

Komatitsch, D., and J. Tromp, 2002, Spectral-element simulations of global seismic wave propagation—i. validation: Geophysical Journal International, **149**, 390–412, doi: https://doi.org/10.1046/j.1365-246X.2002.01653.x.

Masfara, L. O. M., T. Cullison, and C. Weemstra, 2022, An efficient probabilistic workflow for estimating induced earthquake parameters in 3d heterogeneous media: Solid Earth, **13**, 1309–1325, doi: https://doi.org/10.5194/se-13-1309-2022.

Mustac, M., and H. Tkalčić, 2016, Point source moment tensor inversion through a bayesian hierarchical model: Geophysical Journal International, **204**, 311–323, doi: https://doi.org/10.1093/gji/ggv458.

Neal, R. M., 2011, Mcmc using hamiltonian dynamics, Handbook of Markov chain Monte Carlo, **2**, 2.

Smith, J. D., R. S. White, J.-P. Avouac, and S. Bourne, 2020, Probabilistic earthquake locations of induced seismicity in the Groningen region, the Netherlands: Geophysical Journal International, **222**, 507–516, doi: https://doi.org/10.1093/gji/ggaa179.

Willacy, C., E. van Dedem, S. Minisini, J. Li, J.-W. Blokland, I. Das, and A. Droujinine, 2019, Full-waveform event location and moment tensor inversion for induced seismicity: Geophysics, **84**, no. 2, KS39–KS57, doi: https://doi.org/10.1190/geo2018-0212.1.